Published in final edited form as:

Sci Signal. 2023 October 24; 16(808): eabo6555. doi:10.1126/scisignal.abo6555.

Human IL-17A protein production is controlled through a PIP5K1α-dependent translational checkpoint

Shankar K. Revu[1], **Wenjuan Yang**[2], **Dhivyaa Rajasundaram**[3], **Alexander Brady**[2], **Saikat Majumder**[1], **Sarah L. Gaffen**[1], **William Hawse**[4], **Zongqi Xia**[5], **Mandy J. McGeachy**[1,2,*]

[1]Division of Rheumatology, Department of Medicine, University of Pittsburgh, Pittsburgh, PA 15261, USA.

[2]Department of Microbiology and Immunology, Cornell University, Ithaca, NY 14850, USA.

[3]Department of Pediatrics, University of Pittsburgh, Pittsburgh, PA 15261, USA.

[4]Department of Immunology, University of Pittsburgh, Pittsburgh, PA 15261, USA.

[5]Department of Neurology, University of Pittsburgh, Pittsburgh, PA 15261 USA.

Abstract

The cytokine interleukin-17 (IL-17) is secreted by T helper 17 (T_H17) cells and is beneficial for microbial control; however, it also causes inflammation and pathological tissue remodeling in autoimmunity. Hence, T_H17 cell differentiation and IL-17 production must be tightly regulated, but to date, this has been defined only in terms of transcriptional control. Phosphatidylinositols are second messengers produced during T cell activation that transduce signals from the T cell receptor (TCR) and costimulatory receptors at the plasma membrane. Here, we found that phosphatidylinositol(4,5)bisphosphate (PIP_2) was enriched in the nuclei of human T_H17 cells, which depended on the kinase PIP5K1α, and that inhibition of PIP5K1α impaired IL-17A production. In contrast, nuclear PIP_2 enrichment was not observed in T_H1 or T_H2 cells, and these cells did not require PIP5K1α for cytokine production. In T cells from patients with multiple sclerosis, IL-17 production elicited by myelin basic protein was blocked by PIP5K1α inhibition without altering either the abundance or stability of *IL17A* mRNA in T_H17 cells. Instead, analysis of PIP5K1α-interacting proteins revealed that PIP5K1α interacted with ARS2, a nuclear cap-binding complex scaffold protein, to facilitate its binding to *IL17A* mRNA and subsequent IL-17 protein production. These findings highlight a transcription-independent, translation-dependent mechanism for regulating IL-17A protein production that might be relevant to other cytokines.

*Corresponding author. mandymcgeachy@cornell.edu.

Author contributions: S.K.R. performed experiments, data analysis, and helped write the manuscript. W.Y. performed experiments. D.R. performed bioinformatics analysis. A.B. assisted with experiments and provided technical advice. S.M. assisted with experiments and provided technical advice. S.L.G. provided technical expertise and intellectual advice for experiment design and data interpretation. W.H. performed experiments and provided technical expertise and intellectual advice for experiment design with PIP_2 analysis. Z.Q. provided MS samples and clinical expertise. M.J.M. conceived and directed the project, performed data analysis, and wrote the paper.

Competing interests: Z.X. has served as a Consultant for Genentech/Roche. The other authors declare that they have no competing interests.

INTRODUCTION

T helper 17 (T_H17) cells, which produce the cytokine interleukin-17 (IL-17), are a subset of $CD4^+$ T cells best known as drivers of chronic inflammation in autoimmunity[1]. GWAS identified susceptibility loci in multiple T_H17 cell–associated genes, including the gene encoding the interleukin-23 (IL-23) receptor[2], and drugs targeting T_H17 cell function by blocking IL-23 or IL-17A signaling are quite successful in the treatment of psoriasis, psoriatic arthritis, ankylosing spondyloarthropathies, and Crohn's disease[1,2]. Anti–IL-17A antibody showed some efficacy in phase II trials in patients with multiple sclerosis (MS)[3], although further evaluation of this approach is needed, and there are concerns regarding the ability of biologic therapies to penetrate central nervous system (CNS) tissue for efficacy. Because autoimmune disease presents when T cells are already activated, understanding mechanisms that regulate not only the differentiation, but the function of T helper subsets is critical to design improved targeted therapeutics.

Genetic susceptibility studies highlight important roles for cytokine, T cell receptor (TCR), and costimulatory signaling pathways in autoimmune disease, suggesting that perturbations in intracellular signaling could alter thresholds for pathogenic T cell activation and function[4,5]. In the absence of cytokines, TCR signal strength alters the balance between T_H1 and T_H2 cells and between effector T cells and regulatory T (T_{reg}) cells[6,7]. When considering T_H17 cells in health and disease, a common theme is that T_H17 cells arise in response to antigens that would be expected to generate relatively weak signals through the TCR and the costimulatory receptor CD28. Many T cells bearing high-affinity, self-reactive TCRs are deleted in the thymus or become T_{reg} cells[8], and B7 costimulatory molecules are tightly regulated in tolerogenic environments, such as the gut, where many T_H17 cells reside in the healthy state[9]. A few studies suggest that low-strength signals through the TCR and CD28 may favor T_H17 cell development in the presence of cytokines[10–13]. We previously described inhibitory roles for CD28 in human T_H17 cell differentiation, which were mediated by tuning the strength of Akt activation in the presence of IL-23 and IL-1β[14].

Phosphatidylinositols are critical second messengers that are generated downstream of TCR and costimulatory receptor stimulation during T cell differentiation. phosphatidylinositol(3,4,5)trisphosphate ($PIP_{3)}$ is the dominant phosphatidylinositol studied in T cells, due to its well-known role as a signaling intermediate generated by PI3K upon TCR and CD28 engagement. PIP_3 initiates a cascade of signaling that recruits and activates kinases essential for T cell activation, including Akt[15]. Phosphatidylinositol 4,5-disphosphate (PIP_2), is a necessary substrate for the generation of PIP_3 by PI3K. In addition, PIP_2 is hydrolyzed by TCR-activated PLCγ to generate diacylglycerol (DAG) and Ca^{2+}, leading to nuclear factor of activated T cells (NFAT) activation, and NFAT is also required for IL-17 production by T_H17 cells[16,17]. Hence, we reasoned that the PIP_2 concentration at the T cell plasma membrane could be an important regulatory checkpoint for T_H17 cell function, and moreover, that CD28 costimulation may alter PIP_2 to dynamically restrict T_H17 cell differentiation. We therefore sought to determine the concentration and intracellular localization of PIP_2 through imaging approaches. In so doing, we found that human T_H17 cells exhibited enriched nuclear PIP_2 concentrations through the kinase phosphatidylinositol-4-phosphate 5-kinase 1α (PIP5K1α), and uncovered

a previously uncharacterized pathway controlling mRNA transcript processing that regulates the production of IL-17A protein through the nuclear cap binding interacting protein, ARS2.

RESULTS

PIP5K1α generates nuclear PIP_2 and is inhibited by CD28 costimulation in T_H17 cells

T_H17 cells were differentiated in vitro from peripheral blood naïve T cells in the presence or absence of anti-CD28, and PIP_2 was analyzed by imaging flow cytometry. As we predicted, the abundance of PIP_2 in T_H17 cells was reduced by CD28 costimulation and this was reversed by an inhibitor of Akt (Fig. 1A). However, the increased PIP_2 abundance was not found around the plasma membrane. Instead, the imaging analysis revealed an unexpected enrichment of PIP_2 in the nuclei of T_H17 cells, and it was this nuclear PIP_2 that was most substantially reduced in abundance by CD28 costimulation in an Akt-dependent manner (Fig. 1, B and C). Furthermore, T_H17 cells had significantly increased nuclear PIP_2 abundance compared to that in T_H1 and T_H2 cells (Fig. 1D).

Within mammalian cells, PIP_2 is locally concentrated for compartmentalized effects. For example, membrane-proximal PIP_2 serves as a substrate for PI3K and PLCγ, while nuclear PIP_2 is thought to direct RNA polymerase activity and gene expression, although this has not been previously studied in T cells[18,19]. Intracellular compartmentalization of PIP function is achieved by localization of PIP_2-generating enzymes at that site[20,21]. PIP_2 can be generated from PI(4)P by kinases of the PIP5K1 family or from $PI(3,4,5)P_3$ by phosphatases, such as PTEN, which promotes T_H17 differentiation of mouse T cells[22]. However, we found that PTEN inhibition did not reduce IL-17 production by cultured human T_H17 cells (fig. S1A). The kinase PIP5K1γ was similarly not required for IL-17 production (fig. S1B). However, PIP5K1α has previously been associated with the generation of nuclear-compartmentalized PIP_2[19], and we found that inhibition of PIP5K1α abrogated reduced the nuclear abundance of PIP_2 in T_H17 cells (Fig. 1E and fig. S1C). We therefore analyzed *PIP5K1A* expression in T_H17 cells and found that it was reduced by CD28 costimulation in an Akt-dependent manner (Fig. 1F).

PIP5K1α is critical for the differentiation of naive T cells into T_H17 cells but not T_H1 or T_H2 cells

To test whether PIP5K1α was important during T cell subset differentiation, we chemically inhibited PIP5K1α during naïve T cell activation in vitro. Inhibition of PIP5K1α impaired T_H17 cell differentiation, as evidenced by the reduced amounts of IL-17 and RORγt, a transcriptional regulator required for T_H17 cell generation (Fig. 2, A to C, fig. S2, A to D). In contrast, T_H1 and T_H2 cell differentiation did not require PIP5K1α (Fig. 2, A and C, fig. S2E), which, together with the low nuclear abundance of PIP_2 in these cell subsets, suggests that PIP5K1α might be a $T_H17$cell–specific therapeutic target.

When the PIP5K1α inhibitor (iPIP5K1α) was added on day 3 after the initiation of T_H17 cell cultures, RORγt protein was not significantly reduced on day 7, but the percentage of IL-17+ cells and the amount of secreted IL-17 were significantly reduced (Fig. 2D, fig. S2, A to D). IL-17 secretion was also impaired when the PIP5K1α inhibitor was added on day

5 of the culture (Fig. 2E, fig. S2, A to D). These results suggest that T_H17 cell function may be modulated by PIP5K1α both through the regulation of RORγt abundance early in the process, and later through regulation of IL-17A production independently of RORγt.

To confirm that these findings were not due to off-target effects of the PIP5K1α inhibitor, we performed siRNA-mediated knockdown of PIP5K1α in naive CD4+ T cells (Fig. 2F). We found that both IL-17A and RORγt production were significantly reduced. Conversely, overexpression of PIP5K1α resulted in increased RORγt and IL-17A production (Fig. 2G, fig. S2, F and G). Together, these data reveal a role for PIP5K1α-mediated PIP_2 signaling specifically in T_H17 cells, and that was not required for T_H1 or T_H2 cell differentiation.

PIP5K1α is required for myelin antigen–induced IL-17 production in T cells from patients with MS

We next established an assay to test the role of PIP5K1α in a clinically relevant setting. MS is an autoimmune disease driven by myelin-reactive T cells that infiltrate the CNS to induce focal demyelinating inflammatory lesions and associated neurological symptoms. T_H17 cells are increased in number during MS clinical relapse, and neutralization of IL-17 showed promise in early-stage clinical trials for MS [3,23]. We collected blood from consenting patients with clinically confirmed relapsing-remitting MS (RRMS) (table S1). PBMCs were isolated and labeled with eFluor670 to monitor proliferation and then were cultured with human myelin basic protein (MBP). In 16 patient samples for which IL-17A production was significantly induced by MBP, this was reversed with a PIP5K1α inhibitor (Fig. 3, A to C, table S1), without affecting the proliferation of activated T cells as assessed by determining the percentage of $CD40L^+$eFluor− cells (Fig. 3D). However, we did not observe any increased production of IFN-γ in response to MBP in this 10-day assay (Fig. 3E). In a second cohort of MS patients (table S2), we further confirmed that MBP-reactive IL-17 secretion was significantly reduced over a 24-hour period by the PIP5K1α inhibitor (Fig. 3F). The short stimulation period supports a direct effect of iPIP5K1α on IL-17A production rather than effects on the proliferation of MBP-responsive T_H17 cells. The low amount of IFN-γ secreted by these cells after treatment with MBP for 24 hours was also reduced by the PIP5K1α inhibitor (Fig. 3G). Because MBP-dependent cytokine production was below the detection limit of flow cytometry at 24 hours, it was not possible to assess whether this IFN-γ production was associated with T_H17 cells that also produced IL-17 or with T_H1 cells. These data therefore support the potential for therapeutically targeting the PIP5K1α-dependent IL-17A pathway to block autoimmune T_H17 cell function.

PIP5K1α modulates IL-17A production without altering *IL17A* expression

Multiple functions for nuclear PIP_2 have been suggested, including chromatin modification and mRNA processing, particularly splicing[18,19,24]. Indeed, the punctate appearance of PIP_2 staining in T_H17 cells corresponds to previous reports of PIP_2 in nuclear speckles, which are the major sites of mRNA processing[19,24]. We performed RNA-sequencing (RNA-seq) and differential gene expression analysis of T_H17 cells that were treated with vehicle or iPIP5K1α on day 3 of culture. We found that PIP5K1α inhibition caused very few changes in global gene expression and did not alter T_H17 cell signature gene expression (Fig. 4, A and B, fig. S3, A and B). DDX46 is an RNA helicase with roles in splicing, and expression

of the gene encoding DDX46 appeared to be slightly but significantly reduced by iPIP5K1α (Fig. 4A). Given the association between PIP_2 in nuclear speckles and mRNA processing, we analyzed splice variants in the RNA-seq data, but found no differences in mRNA splicing between control and iPIP5K1α–treated cells (fig. S3C). Similarly, iPIP5K1α did not lead to differential expression of long noncoding RNAs (fig. S3D) or microRNAs (fig. S3E). We further confirmed that iPIP5K1α did not alter the amounts of *IL17A* or *RORC* (which encodes RORγt) mRNAs when added on days 0 or 3 of culture as assessed by quantitative PCR analysis of cells from additional donors (Fig. 4C). To ensure that the discordant expression of *IL17A* transcript and protein was not due to the way that these were being separately measured, we analyzed *IL17A* mRNA and IL-17 protein amounts in the same cells by imaging flow cytometry and further confirmed that iPIP5K1α impaired IL-17 protein production without affecting *IL17A* mRNA abundance (Fig. 4, D and E).

At the start of translation, mRNA transcripts associate with several proteins to form the elongation initiation complex, including elongation initiation factor 4G (EIF4G). We found that the abundance of EIF4G was unchanged by iPIP5K1α (fig. S4A). We therefore performed RNA immunoprecipitations to test whether *IL17A* transcripts associated with EIF4G. In the presence of iPIP5K1α, there was a reduction in the amount of *IL17A* mRNA that immunoprecipitated with EIF4G (fig. S4B). This suggests that there could be reduced initiation of translation of *IL17A* mRNAs when PIP5K1α is inhibited.

Cytokines have notoriously unstable mRNA transcripts as a mechanism to prevent inappropriate over-expression. To test whether altered entry into the translation machinery could be explained by the reduced stability of *IL17A* mRNA in absence of PIP5K1α activity, we performed Roadblock qPCR, a process in which newly formed RNA transcripts are labeled to prevent their conversion to cDNA during reverse transcription performed for qPCR analysis. These data indicated that *IL17A* transcripts decayed at similar rates after inhibition of PIP5K1α (Fig. 4F). Together, these data suggest an unanticipated role for PIP5K1α (and, by inference, nuclear PIP_2) in controlling *IL17A* mRNA translation rather than *IL17A* transcription as a mechanism for regulating IL-17 production by human T_H17 cells.

PIP5K1α enhances the binding of ARS2 to *IL17A* transcripts and promotes IL-17A protein production

Because PIP_2 was concentrated in the nucleus, we sought to identify potential nuclear proteins that regulated *IL17A* transcript processing. We took advantage of the fact that PIP5K1α binds to PIP_2-activated targets to achieve localized effects within cellular compartments[19,20,25]. We immunoprecipitated PIP5K1α in TH17 cells from three independent donors and subjected the samples to mass spectrometry, which revealed that Arsenite-resistance protein 2 (ARS2) was enriched with PIP5K1α (table S3). We confirmed the interaction between ARS2 and PIP5K1α by co-immunoprecipitation and Western blotting analysis (Fig. 5A). Furthermore, we observed co-localization of ARS2 and PIP_2 in the nuclei of T_H17 cells but not of T_H1 cells by imaging flow cytometry (Fig. 5B). To test whether ARS2 was required for IL-17 production, we depleted ARS2 by siRNA during

T_H17 cell differentiation. ARS2 depletion impaired the production of IL-17, but not IFN-γ, by the T_H17 cells (Fig. 5C, fig. S5, A and B).

Inhibition of PIP5K1α did not alter the abundance of ARS2 in T_H17 cells (fig. S5C). ARS2 interacts with the nuclear cap-binding complex to influence mRNA sorting in nuclear speckles[26–28]. To determine whether ARS2 interacted with the *IL17A* mRNA complex in a PIP5K1α-dependent manner, we analyzed T_H17 cells by RNA immunoprecipitation followed by qPCR. Indeed, *IL17A* transcripts were enriched in the ARS2 immunoprecipitates compared to the control samples (Fig. 5D), and inhibition of PIP5K1α reduced the association between ARS2 and *IL17A* mRNA (Fig. 5D). In contrast, the trend for interactions between ARS2 and *IFNG* transcripts did not reach statistical significance and was unchanged by iPIP5K1α (Fig. 5E). These data indicate that PIP5K1α regulates *IL17A* mRNA translation through interactions with ARS2 that promote the binding of ARS2 to the *IL17A* mRNA–containing complex.

DISCUSSION

$CD4^+$ helper T cells primarily function through the production of cytokines that act as potent intercellular messengers, and as such, there are multiple mechanisms that regulate cytokine production. Cytokine-encoding mRNA transcripts typically contain long 3'-untranslated regions (UTRs) containing many AU-rich elements and stem-loop structures that render them susceptible to degradative RNA-binding proteins, such as tristetraprolin and Regnase-1, ensuring their transient expression[29]. During immune activation, direct transcription of genes encoding lineage-defining cytokines is increased, and in some cases, this is accompanied by an increase in the abundance of RNA-binding proteins that bind to AREs to prevent degradation, stabilizing cytokine mRNAs. For example, in T_H2 cells, the RNA-binding protein HuR (which is encoded by *Elavl1*) stabilizes the mRNA of T_H2 cytokines as well as of the IL-2R to increase production of their proteins and thus promote T_H2 cell differentiation[30,31]. In T_H17 cells, HuR stabilizes *Il17a* transcripts, and HuR deletion renders mice resistant to induction of EAE, a model of MS[32].

Despite burgeoning discoveries in regulation of gene expression and translation in the immune system, only rare examples of posttranscriptional control of cytokine expression through translation, rather than mRNA stabilization, have been described. IFN-γ is rapidly produced by memory T cells, at least in part because pre-formed transcripts are stored in resting memory cells in a state that represses translation. The RNA-binding protein ZFP36L2 binds to AU-rich elements to block access of *Ifng* mRNAs to ribosomes, but this interaction is rapidly dissociated upon activation of the TCR to promote IFN-γ protein production[33]. A similar translation-repressive role has been described for the binding of GAPDH to *Ifng* transcripts, which is also relieved upon T cell activation when the glycolysis pathway is engaged and recruits GAPDH, freeing mRNAs for translation[34].

Here, we found that T cell activation under T_H17-inducing conditions drove the PIP5K1α-dependent translation of *IL17A* transcripts in differentiating T_H17 cells. It appears that PIPK1α also directs early T_H17 cell differentiation, but we did not investigate the precise mechanisms of RORγt expression and stabilization in this study. We focused on

unraveling the mechanism of *IL17A* regulation, because this is pertinent to therapeutic goals of blocking already established pathogenic T_H17 cell function in autoimmune patients. Although we have not ruled out the possibility that PIP5K1α binds to mRNAs directly, it was a more likely scenario that this kinase would act by altering the function of an additional interacting protein to promote mRNA translation. Our data identified ARS2 as a target of PIP5K1α and showed that the binding of ARS2 to *IL17A* transcripts depended on PIP5K1α activity. ARS2 acts as a scaffold between mRNA, cap-binding proteins, and RNA-binding proteins, and thus can direct interactions with RNA-processing and transport complexes to regulate translation[28]. In this capacity, ARS2 plays a role in the selective processing of mRNA transcripts, and here we have unveiled an additional mechanism by which binding of ARS2 to specific transcripts can be regulated through cell membrane receptor activation.

PIP5K1α is one of three isoforms of PIP5K1 that generate PIP_2 from PIP, together with the phosphatase PTEN that converts PIP_3 to PIP_2. Within the cell, locally distinct concentrations of phosphatidylinositols can be achieved by compartmentalization of the PI-generating kinases. PIP5K1α regulates nuclear PIP_2 concentration. However, PIP5K1α is also recruited to the T cell membrane by CD28 ligation, resulting in the increased production of PIP_2, which acts as a substrate for PI3K, leading to Akt activation[35]. We did not observe any change in T_H1 cell differentiation when PIP5K1α activity was inhibited either in the presence of absence of CD28 costimulation, suggesting some redundancy with other PIP_2-generating enzymes at the cell surface during T helper cell differentiation. However, the recruitment of PIP5K1α to the plasma membrane and away from the nucleus is consistent with our observation that CD28 signaling resulted in reduced nuclear PIP_2 abundance and T_H17 cell differentiation, in addition to reduced expression of *PIP5K1A*.

Note that the activity and requirement for PIP5K1α in the nuclear regulation of T cell function seemed to depend on the milieu of extracellular signals received by the T cell. Under the same conditions of TCR stimulation, cytokines that promoted T_H1 or T_H2 cell differentiation did not require PIP5K1α nor did they stimulate the nuclear accumulation of PIP_2, suggesting that there are alternative mechanisms of TCR/CD28-dependent phosphatidylinositol generation in these cell subsets. We previously showed that CD28 costimulation of already differentiated T_H17 cells does not inhibit their production of IL-17[14]. IL-17 production in response to CD28 costimulation in the absence of TCR ligation, including in samples from people with MS, has also been reported[36–38]. Indeed, this CD28-autonomous induction of IL-17 production is PIP5K1α-dependent[38], consistent with our observation that PIP5K1α promotes IL-17 production during the later phases of T_H17 cell culture and in the recall of autoimmune circulating cells. It is possible that PIP5K1α plays additional roles in driving IL-17 production by memory T_H17 cells through supporting TCR/CD28 signaling in addition to enhancing IL-17A protein production, but this remains to be tested. In this context, it is worth highlighting that CD28 inhibits T_H17 cell generation in a dose-dependent manner when using agonistic anti-CD28 in vitro, and this inhibition can be mitigated by reducing the concentration of anti-CD3[14,39]. In other words, cumulative signals from the TCR and CD28 determine T_H17 cell output, much as has been described for T_H1 and T_H2 cells[14,40]. Hence, studies that use CD28 costimulation as part of the T_H17-polarizing conditions may still observe T_H17 cell differentiation, and T_H17

potential in these cultures may or may not be underestimated depending on the strength of the signal through CD3.

Here, we generated T_H17 cells by stimulating naïve $CD4^+$ T cells in the presence of IL-23 and IL-1β, a cytokine combination thought to drive the proinflammatory phenotype of cells involved in autoimmune disease. Protective, or nonpathogenic, T_H17 cells are present in healthy individuals in barrier sites, including the intestine and skin. These T_H17 cells help to regulate microbiota populations and promote healing without causing overt inflammation[41,42]. Protective resident T_H17 cells have altered metabolic states compared to those of pro-inflammatory T_H17 cells, and it is posited that they are more dependent on IL-6, compared to pro-inflammatory T_H17 cells, which require IL-23[43–45]. In mouse systems, the cytokine TGF-β promotes T_H17 cell differentiation, but high concentrations of TGFβ inhibit pathogenic function in part through increased IL-10 production[46,47]. Although the role of TGFβ in human T_H17 cells remains controversial, it appears to play a minimal role[48–50]. Overall, the costimulatory and cytokine signals received by activated T cells converge to determine their functional outcome, and our data suggest that regulating the translation of transcripts of pathogenic cytokines (in this case, IL-17) is one mechanism by which the magnitude of inflammation induced by T_H17 cells can be modulated downstream of these extracellular signals. Given that this nuclear PIP_2–associated, posttranscriptional pathway is unexplored in the immune system, it will be very interesting in future to determine the role of PIP5K1α and ARS2 in modulating inflammatory responses in other innate and adaptive immune cells, particularly those capable of responding to IL-23 and IL-1β.

MATERIALS AND METHODS

Isolation of human peripheral blood mononuclear cells (PBMCs) and T cells

Whole blood buffy coats from healthy consenting adult donors were obtained from the Pittsburgh Central Blood Bank, Stem Cell Technologies, or the New York Blood Center, and were de-identified for demographics, including age, sex, and race, after approval by the University of Pittsburgh Institutional Review Board and Cornell University Institutional Review Board. Blood samples from subjects with relapsing-remitting MS were obtained from the PROMOTE registry at the University of Pittsburgh, and informed consent was obtained after the nature and possible consequences of possible studies were explained (Institutional Review Board STUDY19080007B). PBMCs were isolated from healthy donor buffy-coats by Ficoll-plague (Sigma-Aldrich) density gradient centrifugation at 400*g* for 30 min at room temperature with no brake. PBMCs were collected and washed twice with PBS by centrifugation at 200*g* for 15 min at 4°C and stored overnight at 4°C in PBS. Naïve $CD4^+$ T cells were separated by negative selection with the human Naïve $CD4^+$ T cell isolation kit II (130–094-131, Miltenyi biotec). Cell purity of >95% was obtained for most of the donors to perform downstream applications.

In vitro cell culture and $CD4^+$ T cell differentiation

Naïve $CD4^+$ T cells were cultured at a density of either 2.5×10^5 cells in 96-well or 1.5×10^6 cells in 24-well culture plates. Cells were activated with plate-bound human

anti-CD3 (5 μg/ml; clone OKT3, BioXcell) and soluble anti-CD28 (2.5 μg/ml; clone CD28.2, Biolegend) in complete RPMI medium supplemented with 10% fetal bovine serum (FBS), 2 mM L-glutamine, 100 U/ml penicillin, 100 μg/ml streptomycin, 50 μM 2-β-mercaptoethanol, HEPES, and sodium pyruvate. For T_H17 cell cultures, 50 ng/ml of recombinant human IL-23 (catalog#1290-IL) and IL-1β (catalog# 201-LB) were added at the initiation of cultures. For T_H1 cultures, 2.5 μg/ml of soluble anti-CD28, 5 ng/ml of recombinant human IL-12 (catalog#219-IL), and 100 U/ml IL-2 were added at the initiation of cultures. All recombinant cytokines were purchased from R&D Systems. Cytokines were analyzed on day 7, and any cultures that showed less than a 50% increase in the concentration of the appropriate cytokine (for example, IL-17, IFNγ, etc.) comparted to that of the negative control (anti-CD3 only, T_H0) was considered to be a technical failure and all data for that donor were excluded (which occurred for <10% of donors). For inhibitor studies, cells were treated with 1.25 μM AKT1/2 inhibitor (Catalog# ab142088, Abcam), 10 μM PIP5K1α inhibitor (catalog#ISA-2011B, MedChemExpress), 10 μM PTEN inhibitor (SF1670 Catalog#5020, Tocris), or 10 μM PIP5K1γ inhibitor (UNC3230, catalog#5271, Tocris) on the days indicated in the figure legends.

Imaging flow cytometry

Cells were cultured under T_H17- or T_H1-polarizing conditions for 5 days before being washed with PBS and then fixed and permeabilized in Foxp3 fixation buffer (catalog#00–5523-00, Invitrogen). Cells were stained with antibodies against the cell surface markers CD4 and CD154. For nuclear staining, biotinylated anti-Ptdlns (4,5)P_2 IgM (1 in 200 dilution, catalog#Z-B045, Echelon Biosciences) and secondary streptavidin-PE was used. Anti-ARS2 (1 in 100 dilution, catalog#NBP2–15473, Novus Biologicals) and FITC-conjugated secondary antibody used. Nuclei were stained with DAPI. To stain cytokine proteins and mRNAs, cells were stimulated with PMA and ionomycin in the presence of GolgiPlug and then fixed and stained with the RNA probe IL17A-AF488 (catalog# VA4–16190-VC, ThermoFisher) and PE-conjugated antibody against IL-17A (clone#N49–653 RUO, BD Biosciences) with the Prime flow RNA kit (catalog#88–18005, ThermoFisher), according to the manufacturer's instructions. Cell imaging analysis was performed by Amnis ImageStream X Imaging flow cytometry (Department of Immunology, University of Pittsburgh). Images were acquired at 60X magnification. A range of 2000 to 5000 $CD4^+$ T cell events were collected and gated on $CD154^+$ cells to analyze the nuclear presence of PIP_2 or ARS2. Matched fluorescent controls were used to generate a compensation matrix across the corresponding image channels. Data were analyzed with IDEAS 6.2 software with features and intensities were measured or scored.

Flow cytometry analysis

Cell surface markers and intracellular cytokines were detected by flow cytometry with the following anti-human antibodies: CD4 (clone RPA-T4, BD Horizon), CD45RO (clone UCHL1, Biolegend), CD154 (clone 24–31, Biolegend) IL-17A (clone N49–653, BD Horizon), IFN-γ (clone B27, Biolegend), and RORγt (clone Q21–559, BD Biosciences). Before staining, the cells were incubated in complete medium with PMA (50 ng/ml) and ionomycin (500 ng/ml, Sigma-Aldrich) and Golgiplug (BD Biosciences) for 4 hours. To exclude dead cells, samples were stained with GhostDye Violet510 (TONBO biosciences).

To stain intracellular cytokines and transcription factors, cells were fixed and permeabilized with the Foxp3 fixation buffer kit (Invitrogen). Samples were collected on a BD LSRII flow cytometer, and data analysis of live $CD4^+CD45RO^+$ or $CD154^+$efluor670− cells and flow cytometry plots were generated with FlowJo software (Treestar).

MBP stimulation assay

Blood was obtained from patients with MS with active disease, and blood from age- and sex-matched healthy donors was taken as controls. PBMCs were isolated from blood as described earlier. Freshly isolated PBMCs were stained with eFluor670 proliferation dye (catalog#65–0840-85, eBioscience) according to the manufacturer's instructions. Total PBMCs were cultured at a density of 2×10^6 cells per well in a 24-well plate with or without human MBP (50 μg/ml, catalog#M0689, Sigma Aldrich), and 10 μM PIP5K1α inhibitor for 10 days. IL-2 (100 U/ml) was added on day 5 after initiation of cultures.

RNA isolation and quantitative real-time PCR (qRT-PCR)

Total RNA was isolated from naïve $CD4^+$ T cells with the RNeasy mini purification Kit (Qiagen), and cDNA was obtained with the High Capacity Reverse Transcription cDNA synthesis kit. qRT-PCR was performed with SYBR Green PCR Master Mix with ROX. The expression of *IL17A* and *IFNG* was normalized to that of the housekeeping gene *B2M*, and *18s* rRNA primers were used from Qiagen RT2 qPCR primer assays. For RNA immunoprecipitation (RIP) analysis, RNA was isolated from bead immune complexes with the PureLink RNA mini kit (catalog#12183018A, Invitrogen). cDNA was synthesized with Superscript IV VILO master mix (catalog#11756050, Invitrogen), and qRT-PCR was performed with Taqman fast advanced master mix (catalog#4444554). Probes were used to detect human *IL17A* (Hs00936345_m1) and human *IFNG* (Hs00989291_m1). Reagents were purchased from Applied Biosystems. The relative amounts of given mRNAs were determined with a 7300 real-time PCR system (Applied Biosystems).

RNA-seq analysis

Isolation of mRNA and library preparation were performed with ultra DNA library prep kits. RNA-seq analysis was performed on an Illumina NextSeq500 with 75-bp single-end reads by the Health Science Sequencing core facility at the University of Pittsburgh. Raw RNA-seq data in fastq format were processed with FastQC, and trimmed reads were aligned with a pipeline that combines STARv.2.7.3a [51] and RSEM version 1.3.2 [52]. Differential expression analysis was implemented with DESeq2 using the read counts derived from RSEM as input. To adjust for the donor variability associated with the sample source, we implemented a multifactor negative binomial model "~Donor + condition," including the donor source to account for the substantial source of variation with DESeq2 [53]. The correction was effective as indicated by the PCA plot of the first two PCs after correction. The Benjamini-Hochberg method was used to correct for multiple testing, and genes were considered to be differentially expressed at an adjusted P value < 0.05. Secondary analyses assessed isoform expression data, which were also quantified with RSEM. The R package NBSplice [54] was used to estimate the differences in the relative expression of gene transcripts between the experimental conditions to infer changes in alternative splicing patterns. For small, noncoding RNA-seq, RNA was isolated with a Nucleospin

kit (Takara), and libraries were prepared with the QIAseq small RNA kit (Qiagen) and sequenced on an Illumina NextSeq500, with >10 million reads per sample obtained. Raw RNA-seq data in fastq format were processed with Partek Flow. After trimming adapters, long noncoding RNAs were filtered based on size >31bp, aligned with Bowtie 2, and quantified to Ensembl hg38. Normalized counts were adjusted for donor batch effect and subjected to GSA analysis with a 1.2-fold cutoff. After correction for multiple testing, no significant differences were observed.

Transfection of cells with siRNAs and plasmids

Freshly isolated, unstimulated naïve $CD4^+$ T cells from human PBMCs were used for nucleofection with an amaxa nucleofector II (Lonza). Nucleofection was performed according to the manufacturer's instructions with amaxa Human T cell nucleofector kit (catalog#VPA-1002, Lonza) and the V-024 program setting for maximal efficiency. ON-TARGETplus SMARTpool siRNAs (500 nM) specific for PIP5K1α (L-004780–00-005) and SRRT (L-019234–01-0005) and the non-targeting control siRNA (D-001810–10-05) were used (Dharmacon). For over-expression experiments, 1 μg of plasmid encoding HA-tagged PIP5K1α or an empty plasmid were used. Plasmid constructs were a kind gift from Richard A. Anderson (University of Wisconsin). After nucleofection, the cells were rested for 2 hours in warm complete RPMI medium. Cells were then plated on anti-CD3–coated 96- or 24-well plates in the presence of T_H17-polarizing cytokines for 7 days.

Roadblock-qPCR mRNA stability assay

T_H17 cell cultures were initiated, and iPIP5K1α was added on day 3. On day 5, Roadblock-qPCR was performed as previously described[55]: 4sU (Sigma-Aldrich) was added for the appropriate times to label cells before they were harvested, washed, and lysed for RNA isolation with a Qiagen RNAeasy Plus Kit. The RNA quality was checked, and up to 1 μg of RNA was subjected to thermal denaturation followed by binding of NEM (Sigma-Aldrich) to 4sU-labeled transcripts. RNA was cleaned with a Zymo RNA Clean and Concentrator kit before undergoing reverse transcription and qPCR analysis of *IL17A* (Taqman) and *18S*rRNA (high abundance ribosomal RNA, Taqman).

Western blotting

Total cell lysates were prepared in Pierce lysis buffer (catalog#87788, ThermoFisher) with protease inhibitors for 15 min at 4°C with rocking. Cells were centrifuged at full speed for 15 min at 4°C and supernatants were collected. Sample buffer (1×) was added to the supernatants, which were then incubated for 5 minutes at 95°C. SDS-PAGE was performed, and proteins were transferred to PVDF membranes, which were blocked with 0.1%TBS/Tween-20, 5% BSA for 1 hour at room temperature. The membrane was incubated with anti-PIP5K1α (catalog# 9693S, Cell signaling Technology), anti-ARS2 (catalog#NBP2–15473, Novus Biologicals), and anti–β-actin (catalog#5125S, Cell Signaling Technology) overnight at 4°C. The blots were then incubated with HRP-conjugated secondary antibody at room temperature for 1 hour. Membranes were developed with the Pierce ECL kit. Protein bands were visualized with FluorChem E detection system.

IP-MS

Protein lysates were extracted from T_H17 cells on day 6 of culture and incubated with anti-PIP5K1α (catalog# sc-398687, clone F-4, Santa Cruz) or IgG isotype control overnight at 4°C. Immune complexes were pulled down with Protein G agarose beads (catalog#11719416001, Roche) for 6 hours at 4°C. Bead-bound immune complexes were stored at −80°C until samples were subjected to protein profiling. Western blotting was performed to confirm the presence of PIP5K1α before the samples were subjected to MS analysis. Samples were eluted in 70 μl of 1.5X LDS buffer at 100°C for 15 min. Samples were clarified by centrifugation and resolved by SDS-PAGE on a 10% Bis-Tris NuPage Mini-gel (Invitrogen) with the MES buffer system. The gel was run for 2 cm. The mobility region was excised into 10 equally sized bands. Each band was processed by in-gel digestion with trypsin (ProGest, DigiLab). Half of each digested sample was analyzed by nano-scale LC-MS/MS with a Waters M-Class LC system interfaced to a ThermoFisher Fusion Lumos mass spectrometer. Peptides were loaded onto a trapping column and eluted over a 75-μm analytical column at 350 nl/min; both columns were packed with Luna C18 resin (Phenomenex). The mass spectrometer was operated in data-dependent mode, with the Orbitrap operating at 60,000 and 15,000 FWHM for MS and MS/MS, respectively. The instrument was run with a 3-s cycle for MS and MS/MS. Five hours of total instrument time was used for the analysis of each submitted sample. Data were searched with a local copy of Mascot (Matrix Science) with the following parameters: Enzyme: Trypsin/PDatabase: SwissProt Human(concatenatedforward and reverse plus common contaminants). Fixed modification: Carbamidomethyl Variable modifications: Oxidation (M), Acetyl (N-term), Pyro-Glu (N-term Q), Deamidation (N/Q)Mass values: Monoisotopic Peptide Mass Tolerance: 10 ppm Fragment Mass Tolerance: 0.02 DaMax Missed Cleavages: 2. Mascot DAT files were parsed into Scaffold (Proteome Software) for validation, filtering, and to generate a nonredundant listper sample. Data were filtered at 1% protein and peptide FDR and requiring at least two unique peptides per protein with a > three-fold increase in PIP5K1α-IP over the IgG control.

RNA immunoprecipitation

Naïve $CD4^+$ T cells were cultured in the presence of T_H17-polarizing cytokines for 6 days. On day 3, PIP5K1α inhibitor was added. Cells were then washed in PBS and lysed in Pierce IP lysis buffer (catalog#87787, ThermoFisher) with RNase and protease inhibitors. Supernatants were collected and subjected to immunoprecipitation with anti-ARS2 (B-11) (catalog# sc-376716, Santa Cruz Biotechnology) or IgG Isotype control antibody (catalog#401402, clone MG1–45, Biolegend) by incubation overnight at 4°C with rocking. Protein G agarose beads were used to pull down immune complexes for 4 to 6 hours at 4°C with rocking. Bead complexes were subjected to RNA isolation as described earlier.

ELISA

Cell culture medium was analyzed to detect secreted cytokines. The culture medium was assayed by ELISA with the Ready-SET-Go kits for human IL17A (catalog#88–7176-88) and IFN-γ (88–7316-88, eBioscience) according to the manufacturer’s instructions. Samples

were stored at −20°C until needed for the assay. All samples were analyzed in duplicate from independent experiments.

Statistical analysis

Statistical analysis was performed by one-way analysis of variance (ANOVA) with multiple comparisons or by Student's *t* test for comparison of two groups. Statistically significant *P* values are indicated in the figure legends as follows: $*P < 0.05$, $**P < 0.01$, $***P < 0.001$, and $****P < 0.0001$. Data are means of multiple donors, and error bars represent the SD.

Supplementary Material

Refer to Web version on PubMed Central for supplementary material.

Acknowledgments:

Authors acknowledge assistance from the Health Sciences at ChP sequencing core, particularly W. MacDonald and A. Poholek, and the Unified flow cytometry core for flow cytometry and Imagestream, and assistance from the E. Mudrak in the Cornell Statistical Consulting Unit. We thank the patients participating in the PROMISE registry at the University of Pittsburgh. We thank R. Anderson, University of Wisconsin, for generous provision of the HA-PIP5K1α plasmid construct. We thank R. Bechara, N. Ponde, L. Kane, and P. Biswas for technical advice and helpful discussions.

Funding:

This study was funded by a University of Pittsburgh PACER award (M.J.M.); the Rheumatology Research Foundation (M.J.M.); NIH AI148356 (M.J.M.); NIH R01NS098023, NIH R01NS124882, and NIH U24NS107166 (Z.X.); and NIH AI147383 (S.L.G.).

Data and materials availability:

Raw and processed RNA-seq data from this study have been deposited under NCBI Gene Expression Omnibus (GEO) under accession code GSE232436. MS data have been deposited in the Proteomics Identifications Database (PRIDE) under accession code MSV000093068. All data needed to evaluate the conclusions in the paper are present in the paper or the Supplementary Materials.

References and Notes

1. Gaffen SL, Jain R, Garg AV, and Cua DJ (2014). The IL-23-IL-17 immune axis: from mechanisms to therapeutic testing. Nat Rev Immunol 14, 585–600. 10.1038/nri3707. [PubMed: 25145755]
2. Patel DD, and Kuchroo VK (2015). Th17 Cell Pathway in Human Immunity: Lessons from Genetics and Therapeutic Interventions. Immunity 43, 1040–1051. 10.1016/j.immuni.2015.12.003. [PubMed: 26682981]
3. Havrdova E, Belova A, Goloborodko A, Tisserant A, Wright A, Wallstroem E, Garren H, Maguire RP, and Johns DR (2016). Activity of secukinumab, an anti-IL-17A antibody, on brain lesions in RRMS: results from a randomized, proof-of-concept study. J Neurol 263, 1287–1295. 10.1007/s00415-016-8128-x. [PubMed: 27142710]
4. Okada Y, Wu D, Trynka G, Raj T, Terao C, Ikari K, Kochi Y, Ohmura K, Suzuki A, Yoshida S, et al. (2014). Genetics of rheumatoid arthritis contributes to biology and drug discovery. Nature 506, 376–381. 10.1038/nature12873. [PubMed: 24390342]
5. Maier LM, and Hafler DA (2009). Autoimmunity risk alleles in costimulation pathways. Immunol Rev 229, 322–336. 10.1111/j.1600-065X.2009.00777.x. [PubMed: 19426231]

6. Hawse WF, Sheehan RP, Miskov-Zivanov N, Menk AV, Kane LP, Faeder JR, and Morel PA (2015). Cutting Edge: Differential Regulation of PTEN by TCR, Akt, and FoxO1 Controls CD4+ T Cell Fate Decisions. J Immunol 194, 4615–4619. 10.4049/jimmunol.1402554. [PubMed: 25855357]
7. Tubo NJ, and Jenkins MK (2014). TCR signal quantity and quality in CD4+ T cell differentiation. Trends Immunol 35, 591–596. 10.1016/j.it.2014.09.008. [PubMed: 25457838]
8. Hogquist KA, Baldwin TA, and Jameson SC (2005). Central tolerance: learning self-control in the thymus. Nat Rev Immunol 5, 772–782. 10.1038/nri1707. [PubMed: 16200080]
9. Mowat AM (2003). Anatomical basis of tolerance and immunity to intestinal antigens. Nat Rev Immunol 3, 331–341. 10.1038/nri1057. [PubMed: 12669023]
10. Ying H, Yang L, Qiao G, Li Z, Zhang L, Yin F, Xie D, and Zhang J. (2010). Cutting edge: CTLA-4--B7 interaction suppresses Th17 cell differentiation. J Immunol 185, 1375–1378. 10.4049/jimmunol.0903369. [PubMed: 20601598]
11. Purvis HA, Stoop JN, Mann J, Woods S, Kozijn AE, Hambleton S, Robinson JH, Isaacs JD, Anderson AE, and Hilkens CM (2010). Low-strength T-cell activation promotes Th17 responses. Blood 116, 4829–4837. 10.1182/blood-2010-03-272153. [PubMed: 20713963]
12. Xin L, Jiang TT, Chaturvedi V, Kinder JM, Ertelt JM, Rowe JH, Steinbrecher KA, and Way SS (2014). Commensal microbes drive intestinal inflammation by IL-17-producing CD4+ T cells through ICOSL and OX40L costimulation in the absence of B7–1 and B7–2. Proc Natl Acad Sci U S A 111, 10672–10677. 10.1073/pnas.1402336111. [PubMed: 25002484]
13. Bouguermouh S, Fortin G, Baba N, Rubio M, and Sarfati M. (2009). CD28 costimulation down regulates Th17 development. PLoS One 4, e5087. 10.1371/journal.pone.0005087. [PubMed: 19333372]
14. Revu S, Wu J, Henkel M, Rittenhouse N, Menk A, Delgoffe GM, Poholek AC, and McGeachy MJ (2018). IL-23 and IL-1beta Drive Human Th17 Cell Differentiation and Metabolic Reprogramming in Absence of CD28 Costimulation. Cell Rep 22, 2642–2653. 10.1016/j.celrep.2018.02.044. [PubMed: 29514093]
15. Scheid MP, Marignani PA, and Woodgett JR (2002). Multiple phosphoinositide 3-kinase-dependent steps in activation of protein kinase B. Mol Cell Biol 22, 6247–6260. [PubMed: 12167717]
16. Gomez-Rodriguez J, Wohlfert EA, Handon R, Meylan F, Wu JZ, Anderson SM, Kirby MR, Belkaid Y, and Schwartzberg PL (2014). Itk-mediated integration of T cell receptor and cytokine signaling regulates the balance between Th17 and regulatory T cells. J Exp Med 211, 529–543. 10.1084/jem.20131459. [PubMed: 24534190]
17. Liu XK, Lin X, and Gaffen SL (2004). Crucial role for nuclear factor of activated T cells in T cell receptor-mediated regulation of human interleukin-17. J Biol Chem 279, 52762–52771. 10.1074/jbc.M405764200. [PubMed: 15459204]
18. Hamann BL, and Blind RD (2018). Nuclear phosphoinositide regulation of chromatin. J Cell Physiol 233, 107–123. 10.1002/jcp.25886. [PubMed: 28256711]
19. Barlow CA, Laishram RS, and Anderson RA (2010). Nuclear phosphoinositides: a signaling enigma wrapped in a compartmental conundrum. Trends Cell Biol 20, 25–35. 10.1016/j.tcb.2009.09.009. [PubMed: 19846310]
20. Choi S, Thapa N, Tan X, Hedman AC, and Anderson RA (2015). PIP kinases define PI4,5P(2)signaling specificity by association with effectors. Biochim Biophys Acta 1851, 711–723. 10.1016/j.bbalip.2015.01.009. [PubMed: 25617736]
21. Sun Y, Thapa N, Hedman AC, and Anderson RA (2013). Phosphatidylinositol 4,5-bisphosphate: targeted production and signaling. Bioessays 35, 513–522. 10.1002/bies.201200171. [PubMed: 23575577]
22. Kim HS, Jang SW, Lee W, Kim K, Sohn H, Hwang SS, and Lee GR (2017). PTEN drives Th17 cell differentiation by preventing IL-2 production. J Exp Med 214, 3381–3398. 10.1084/jem.20170523. [PubMed: 29018045]
23. Kebir H, Ifergan I, Alvarez JI, Bernard M, Poirier J, Arbour N, Duquette P, and Prat A. (2009). Preferential recruitment of interferon-gamma-expressing TH17 cells in multiple sclerosis. Ann Neurol 66, 390–402. 10.1002/ana.21748. [PubMed: 19810097]

24. Galganski L, Urbanek MO, and Krzyzosiak WJ (2017). Nuclear speckles: molecular organization, biological function and role in disease. Nucleic Acids Res 45, 10350–10368. 10.1093/nar/gkx759. [PubMed: 28977640]
25. Schramp M, Hedman A, Li W, Tan X, and Anderson R. (2012). PIP kinases from the cell membrane to the nucleus. Subcell Biochem 58, 25–59. 10.1007/978-94-007-3012-0_2. [PubMed: 22403073]
26. Hallais M, Pontvianne F, Andersen PR, Clerici M, Lener D, Benbahouche Nel H, Gostan T, Vandermoere F, Robert MC, Cusack S, et al. (2013). CBC-ARS2 stimulates 3'-end maturation of multiple RNA families and favors cap-proximal processing. Nat Struct Mol Biol 20, 1358–1366. 10.1038/nsmb.2720. [PubMed: 24270878]
27. Andersen PR, Domanski M, Kristiansen MS, Storvall H, Ntini E, Verheggen C, Schein A, Bunkenborg J, Poser I, Hallais M, et al. (2013). The human cap-binding complex is functionally connected to the nuclear RNA exosome. Nat Struct Mol Biol 20, 1367–1376. 10.1038/nsmb.2703. [PubMed: 24270879]
28. Schulze WM, Stein F, Rettel M, Nanao M, and Cusack S. (2018). Structural analysis of human ARS2 as a platform for co-transcriptional RNA sorting. Nat Commun 9, 1701. 10.1038/s41467-018-04142-7. [PubMed: 29703953]
29. Fu M, and Blackshear PJ (2017). RNA-binding proteins in immune regulation: a focus on CCCH zinc finger proteins. Nat Rev Immunol 17, 130–143. 10.1038/nri.2016.129. [PubMed: 27990022]
30. Techasintana P, Ellis JS, Glascock J, Gubin MM, Ridenhour SE, Magee JD, Hart ML, Yao P, Zhou H, Whitney MS, et al. (2017). The RNA-Binding Protein HuR Posttranscriptionally Regulates IL-2 Homeostasis and CD4(+) Th2 Differentiation. Immunohorizons 1, 109–123. 10.4049/immunohorizons.1700017. [PubMed: 30035254]
31. Casolaro V, Fang X, Tancowny B, Fan J, Wu F, Srikantan S, Asaki SY, De Fanis U, Huang SK, Gorospe M, et al. (2008). Posttranscriptional regulation of IL-13 in T cells: role of the RNA-binding protein HuR. J Allergy Clin Immunol 121, 853–859 e854. 10.1016/j.jaci.2007.12.1166. [PubMed: 18279945]
32. Chen J, Cascio J, Magee JD, Techasintana P, Gubin MM, Dahm GM, Calaluce R, Yu S, and Atasoy U. (2013). Posttranscriptional gene regulation of IL-17 by the RNA-binding protein HuR is required for initiation of experimental autoimmune encephalomyelitis. J Immunol 191, 5441–5450. 10.4049/jimmunol.1301188. [PubMed: 24166976]
33. Salerno F, Engels S, van den Biggelaar M, van Alphen FPJ, Guislain A, Zhao W, Hodge DL, Bell SE, Medema JP, von Lindern M, et al. (2018). Translational repression of pre-formed cytokine-encoding mRNA prevents chronic activation of memory T cells. Nat Immunol 19, 828–837. 10.1038/s41590-018-0155-6. [PubMed: 29988089]
34. Chang CH, Curtis JD, Maggi LB Jr., Faubert B, Villarino AV, O'Sullivan D, Huang SC, van der Windt GJ, Blagih J, Qiu J, et al. (2013). Posttranscriptional control of T cell effector function by aerobic glycolysis. Cell 153, 1239–1251. 10.1016/j.cell.2013.05.016. [PubMed: 23746840]
35. Muscolini M, Camperio C, Porciello N, Caristi S, Capuano C, Viola A, Galandrini R, and Tuosto L. (2015). Phosphatidylinositol 4-phosphate 5-kinase alpha and Vav1 mutual cooperation in CD28-mediated actin remodeling and signaling functions. J Immunol 194, 1323–1333. 10.4049/jimmunol.1401643. [PubMed: 25539813]
36. Kunkl M, Mastrogiovanni M, Porciello N, Caristi S, Monteleone E, Arcieri S, and Tuosto L. (2019). CD28 Individual Signaling Up-regulates Human IL-17A Expression by Promoting the Recruitment of RelA/NF-kappaB and STAT3 Transcription Factors on the Proximal Promoter. Front Immunol 10, 864. 10.3389/fimmu.2019.00864. [PubMed: 31068940]
37. Kunkl M, Porciello N, Mastrogiovanni M, Capuano C, Lucantoni F, Moretti C, Persson JL, Galandrini R, Buzzetti R, and Tuosto L. (2017). ISA-2011B, a Phosphatidylinositol 4-Phosphate 5-Kinase alpha Inhibitor, Impairs CD28-Dependent Costimulatory and Pro-inflammatory Signals in Human T Lymphocytes. Front Immunol 8, 502. 10.3389/fimmu.2017.00502. [PubMed: 28491063]
38. Camperio C, Muscolini M, Volpe E, Di Mitri D, Mechelli R, Buscarinu MC, Ruggieri S, Piccolella E, Salvetti M, Gasperini C, et al. (2014). CD28 ligation in the absence of TCR stimulation up-regulates IL-17A and pro-inflammatory cytokines in relapsing-remitting multiple sclerosis T lymphocytes. Immunol Lett 158, 134–142. 10.1016/j.imlet.2013.12.020. [PubMed: 24412596]

39. Wyatt MM, Huff LW, Nelson MH, Neal LR, Medvec AR, Rangel Rivera GO, Smith AS, Rivera Reyes AM, Knochelmann HM, Riley JL, et al. (2023). Augmenting TCR signal strength and ICOS costimulation results in metabolically fit and therapeutically potent human CAR Th17 cells. Mol Ther 31, 2120–2131. 10.1016/j.ymthe.2023.04.010. [PubMed: 37081789]
40. Bhattacharyya ND, and Feng CG (2020). Regulation of T Helper Cell Fate by TCR Signal Strength. Front Immunol 11, 624. 10.3389/fimmu.2020.00624. [PubMed: 32508803]
41. Stacy A, and Belkaid Y. (2019). Microbial guardians of skin health. Science 363, 227–228. 10.1126/science.aat4326. [PubMed: 30655428]
42. Honda K, and Littman DR (2016). The microbiota in adaptive immune homeostasis and disease. Nature 535, 75–84. 10.1038/nature18848. [PubMed: 27383982]
43. Omenetti S, Bussi C, Metidji A, Iseppon A, Lee S, Tolaini M, Li Y, Kelly G, Chakravarty P, Shoaie S, et al. (2019). The Intestine Harbors Functionally Distinct Homeostatic Tissue-Resident and Inflammatory Th17 Cells. Immunity 51, 77–89 e76. 10.1016/j.immuni.2019.05.004. [PubMed: 31229354]
44. Wu L, Hollinshead KER, Hao Y, Au C, Kroehling L, Ng C, Lin WY, Li D, Silva HM, Shin J, et al. (2020). Niche-Selective Inhibition of Pathogenic Th17 Cells by Targeting Metabolic Redundancy. Cell 182, 641–654 e620. 10.1016/j.cell.2020.06.014. [PubMed: 32615085]
45. Sano T, Kageyama T, Fang V, Kedmi R, Martinez CS, Talbot J, Chen A, Cabrera I, Gorshko O, Kurakake R, et al. (2021). Redundant cytokine requirement for intestinal microbiota-induced Th17 cell differentiation in draining lymph nodes. Cell Rep 36, 109608. 10.1016/j.celrep.2021.109608.
46. McGeachy MJ, Bak-Jensen KS, Chen Y, Tato CM, Blumenschein W, McClanahan T, and Cua DJ (2007). TGF-beta and IL-6 drive the production of IL-17 and IL-10 by T cells and restrain T(H)-17 cell-mediated pathology. Nat Immunol 8, 1390–1397. 10.1038/ni1539. [PubMed: 17994024]
47. Ghoreschi K, Laurence A, Yang XP, Tato CM, McGeachy MJ, Konkel JE, Ramos HL, Wei L, Davidson TS, Bouladoux N, et al. (2010). Generation of pathogenic T(H)17 cells in the absence of TGF-beta signalling. Nature 467, 967–971. 10.1038/nature09447. [PubMed: 20962846]
48. Acosta-Rodriguez EV, Napolitani G, Lanzavecchia A, and Sallusto F. (2007). Interleukins 1beta and 6 but not transforming growth factor-beta are essential for the differentiation of interleukin 17-producing human T helper cells. Nat Immunol 8, 942–949. 10.1038/ni1496. [PubMed: 17676045]
49. Manel N, Unutmaz D, and Littman DR (2008). The differentiation of human T(H)-17 cells requires transforming growth factor-beta and induction of the nuclear receptor RORgammat. Nat Immunol 9, 641–649. 10.1038/ni.1610. [PubMed: 18454151]
50. Volpe E, Servant N, Zollinger R, Bogiatzi SI, Hupe P, Barillot E, and Soumelis V. (2008). A critical function for transforming growth factor-beta, interleukin 23 and proinflammatory cytokines in driving and modulating human T(H)-17 responses. Nat Immunol 9, 650–657. 10.1038/ni.1613. [PubMed: 18454150]
51. Dobin A, Davis CA, Schlesinger F, Drenkow J, Zaleski C, Jha S, Batut P, Chaisson M, and Gingeras TR (2013). STAR: ultrafast universal RNA-seq aligner. Bioinformatics 29, 15–21. 10.1093/bioinformatics/bts635. [PubMed: 23104886]
52. Li B, and Dewey CN (2011). RSEM: accurate transcript quantification from RNA-Seq data with or without a reference genome. BMC Bioinformatics 12, 323. 10.1186/1471-2105-12-323. [PubMed: 21816040]
53. Love MI, Huber W, and Anders S. (2014). Moderated estimation of fold change and dispersion for RNA-seq data with DESeq2. Genome Biol 15, 550. 10.1186/s13059-014-0550-8. [PubMed: 25516281]
54. Merino GA, and Fernandez EA (2020). Differential splicing analysis based on isoforms expression with NBSplice. J Biomed Inform 103, 103378. 10.1016/j.jbi.2020.103378.
55. Watson MJ, and Thoreen CC (2022). Measuring mRNA Decay with Roadblock-qPCR. Curr Protoc 2, e344. 10.1002/cpz1.344. [PubMed: 35041257]

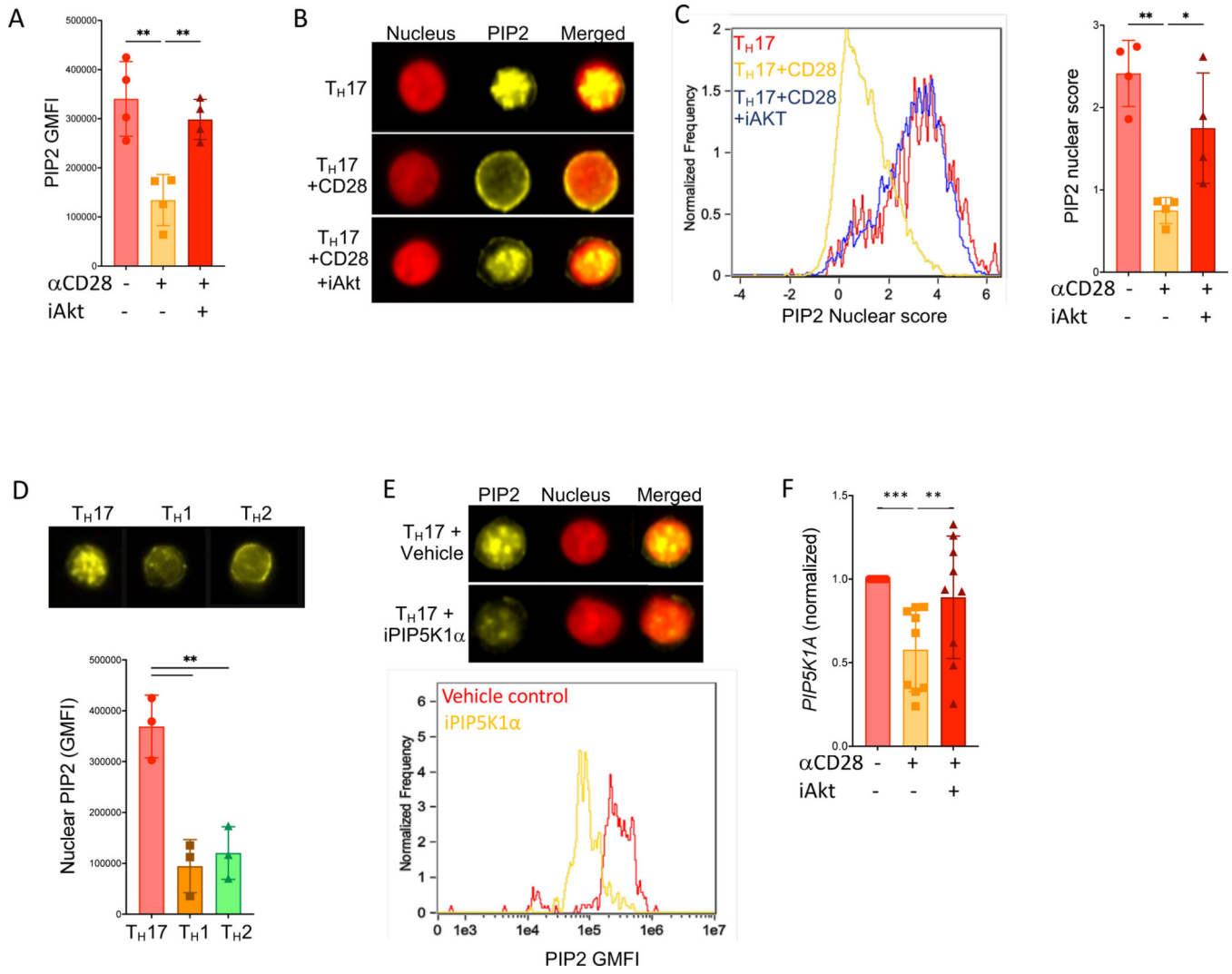

Fig. 1. PIP5K1α stimulates the nuclear accumulation of PIP_2 in T_H17 cells.

(**A** to **C**) Naïve human $CD4^+$ T cells were cultured with anti-CD3, IL-23, and IL-1β (T_H17-inducing conditions) in presence or absence of agonistic anti-CD28 antibody (αCD28) and iAkt as indicated and were analyzed on day 5. (A) PIP_2 expression measured as GMFI from ~1000 cells by imaging flow cytometry. Data are from four donors. (B) Representative images showing PIP_2 as assessed by imaging flow cytometry. (C) Nuclear score of PIP_2 staining in ~1000 cells per condition. Left: Representative histogram. Right: Pooled data from four donors. (**D**) Naïve $CD4^+$ T cells were activated with anti-CD3, IL-23, and IL-1β (T_H17 conditions), IL-12 and IL-2 (T_H1 conditions), or IL-4, IL-2, and anti–IFN-γ (T_H2 conditions) and were analyzed by imaging flow cytometry on day 5. Top: Representative images of nuclear PIP_2. Bottom: Mean GMFI values for nuclear PIP_2 in cells from three donors. (**E**) T_H17 cells were treated vehicle or iPIP5K1α and were analyzed by imaging flow cytometry on day x. Top: Representative images for PIP_2 staining. Bottom: Histogram overlay of the PIP_2 GMFI in ~1000 cells from each condition. Data are representative of four donors. (**F**) T_H17 cells cultured for five days with or without αCD28 and iAkt, as indicated, were analyzed by qPCR to determine the relative expression of *PIP5K1A*

normalized to that of *B2M*. Data are from nine donors. Statistical analysis was performed by one-way ANOVA with multiple comparisons or by Student's *t* test for comparison of two groups. Data are means ± SD. *$P < 0.05$, **$P < 0.01$.

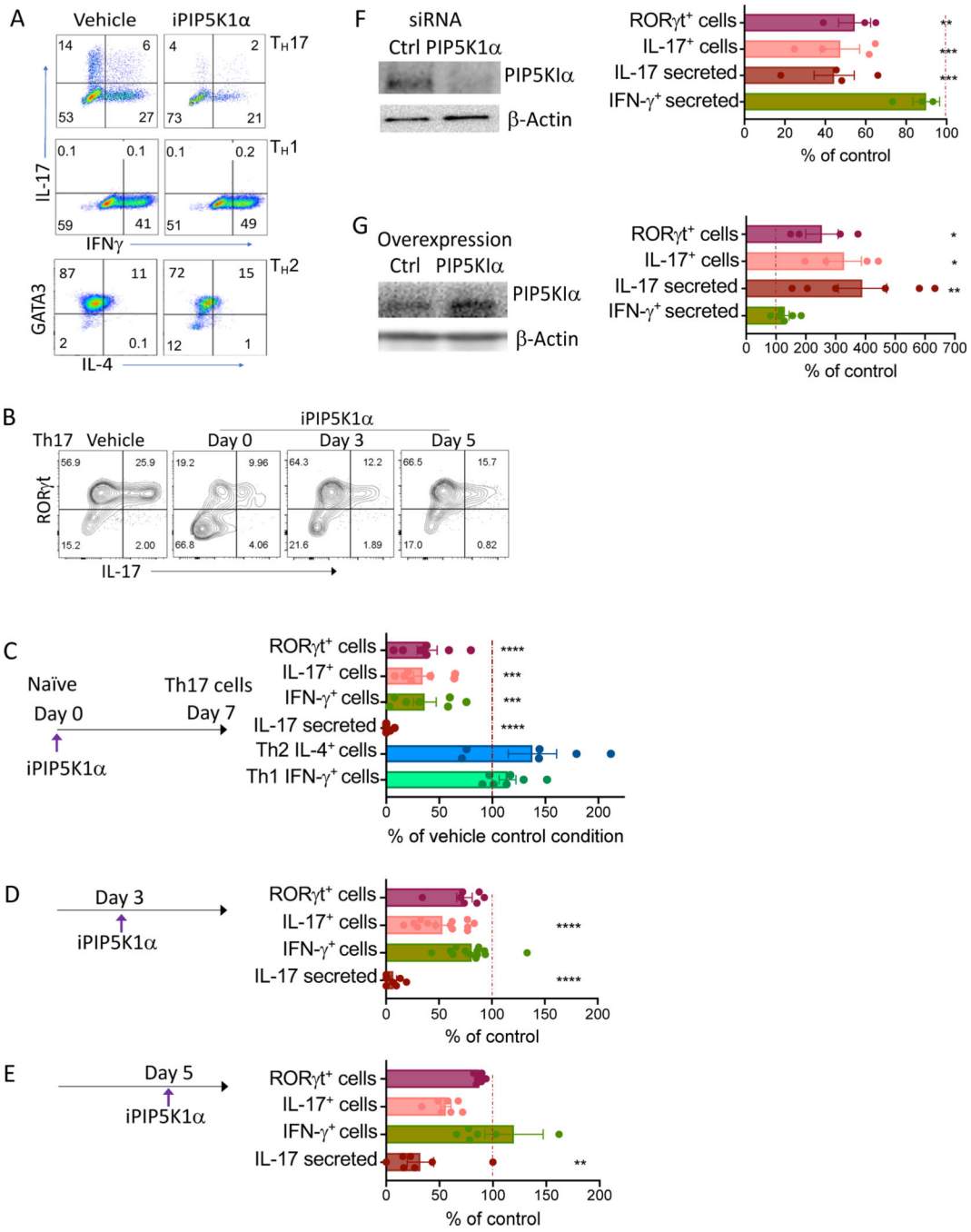

Fig. 2. PIP5K1α is required for the differentiation of T_H17 cells but not T_H1 or T_H2 cells.

(**A** to **E**) Naïve human $CD4^+$ T cells were activated with anti-CD3, IL-23, and IL-1β (T_H17), IL-12 and IL-2 (T_H1), or IL-4, IL-2, and anti–IFN-γ (T_H2) in the presence of iPIP5K1α or vehicle, and cytokine production was analyzed on day 7 of culture. (A) Representative flow cytometry plots for subset-representative cytokines. iPIP5K1α added on day 0. (B) Representative flow cytometry plots from T_H17 cultures in which iPIP5K1α was added at the indicated times and analysis was performed on day 7. (C to E) The indicated cell cultures were treated with vehicle or iPIP5K1a at the indicated times. On day 7, the cells

were analyzed by flow cytometry to determine the percentages of cells positive for the indicated factors or cultures were analyzed by ELISA to determine the amounts of secreted IL-17. Data are from seven donors, except for (D), where data are from 13 donors for IL-17$^+$ and IFNγ^+ cells. (**F**) Naive CD4$^+$ T cells were transfected with PIP5K1α-specific siRNA or scrambled control (Dharmacon) by nucleofection (Amaxa), followed by T_H17 cell differentiation. Left: After 48 hours, PIP5K1α was analyzed by Western blotting. Right: The amounts of the indicated cytokines secreted by the cells were determined by ELISA and the numbers of IL-17$^+$ cells and RORγt$^+$ cells were determined by flow cytometry on day 7. Data are from three or four donors. (**G**) Naive T cells were transfected with HA-PIP5K1α or HA-vector alone. Left: After 48 hours, PIP5K1α was analyzed by Western blotting. Right: The amounts of the indicated cytokines secreted by the cells were determined by ELISA and the numbers of IL-17$^+$ cells and RORγt$^+$ cells were determined by flow cytometry on day 7. Data are from four to six donors. In all graphs, dots represent individual donors, and values for treatments were normalized as a percentage of the control conditions. Data were analyzed by one-sample *t* test against the hypothesized mean. *$P < 0.05$, **$P < 0.01$, ***$P < 0.001$, and ****$P < 0.0001$.

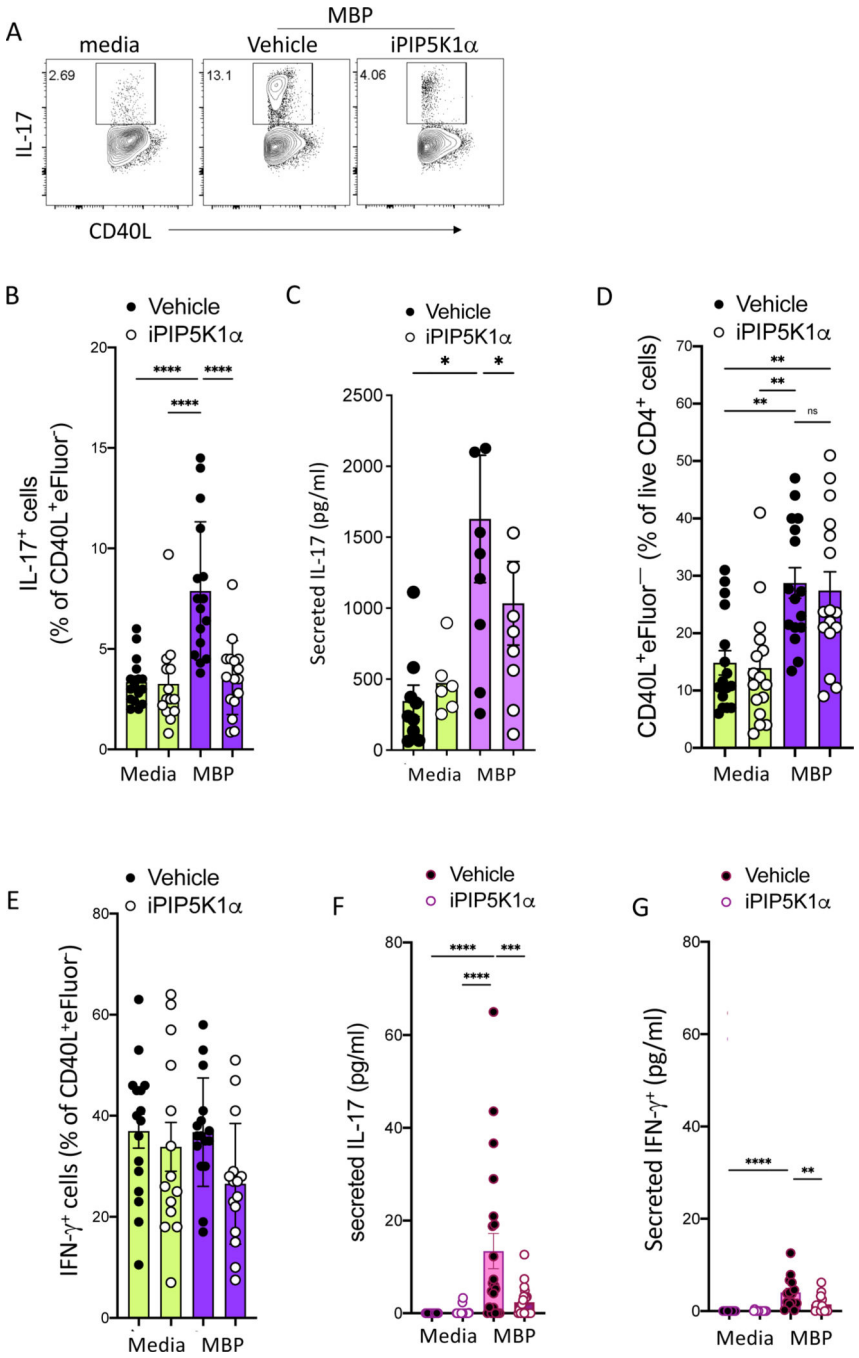

Fig. 3. PIP5K1α inhibition blocks IL-17 production by T_H17 cells from patients with MS.

(**A** to **E**) Freshly isolated PBMCs from patients with relapsing-remitting MS were labeled with the proliferation dye eFluor647 and cultured with MBP in the presence or absence of iPIP5K1α for 10 days. (A) Cells were stimulated with PMA and ionomycin and then analyzed for the indicated intracellular cytokines by flow cytometry after gating on live $CD4^+CD40L^+eFluor-$ cells. (B) The percentages of $IL\text{-}17^+$ cells were determined. (C) The amounts of IL-17 secreted by the indicated cells were determined by ELISA. (D) Cell proliferation was analyzed by flow cytometry. (E) The percentages of IFN-γ^+ cells under the

indicated conditions were determined. (**F** and **G**) Freshly isolated PBMCs from patients with relapsing-remitting MS were cultured with MBP in the presence or absence of iPIP5K1α for 24 hours. The amounts of IL-17 (F) and IFN-γ (G) secreted by the cells were determined by ELISA. The data were background-corrected by subtracting the cytokine amounts for the media controls for each donor. Dots represent individual donors. Demographic information for the donors can be found in tables S1 and S2. Data in (A to E) are pooled data from 16 individual donors. Data in (F and G) are pooled data from 21 individual donors. Statistical analysis was performed by one-way ANOVA with multiple comparisons. Data are means ± SD. $*P < 0.05$, $**P < 0.01$, $***P < 0.001$, and $****P < 0.0001$; ns, not significant.

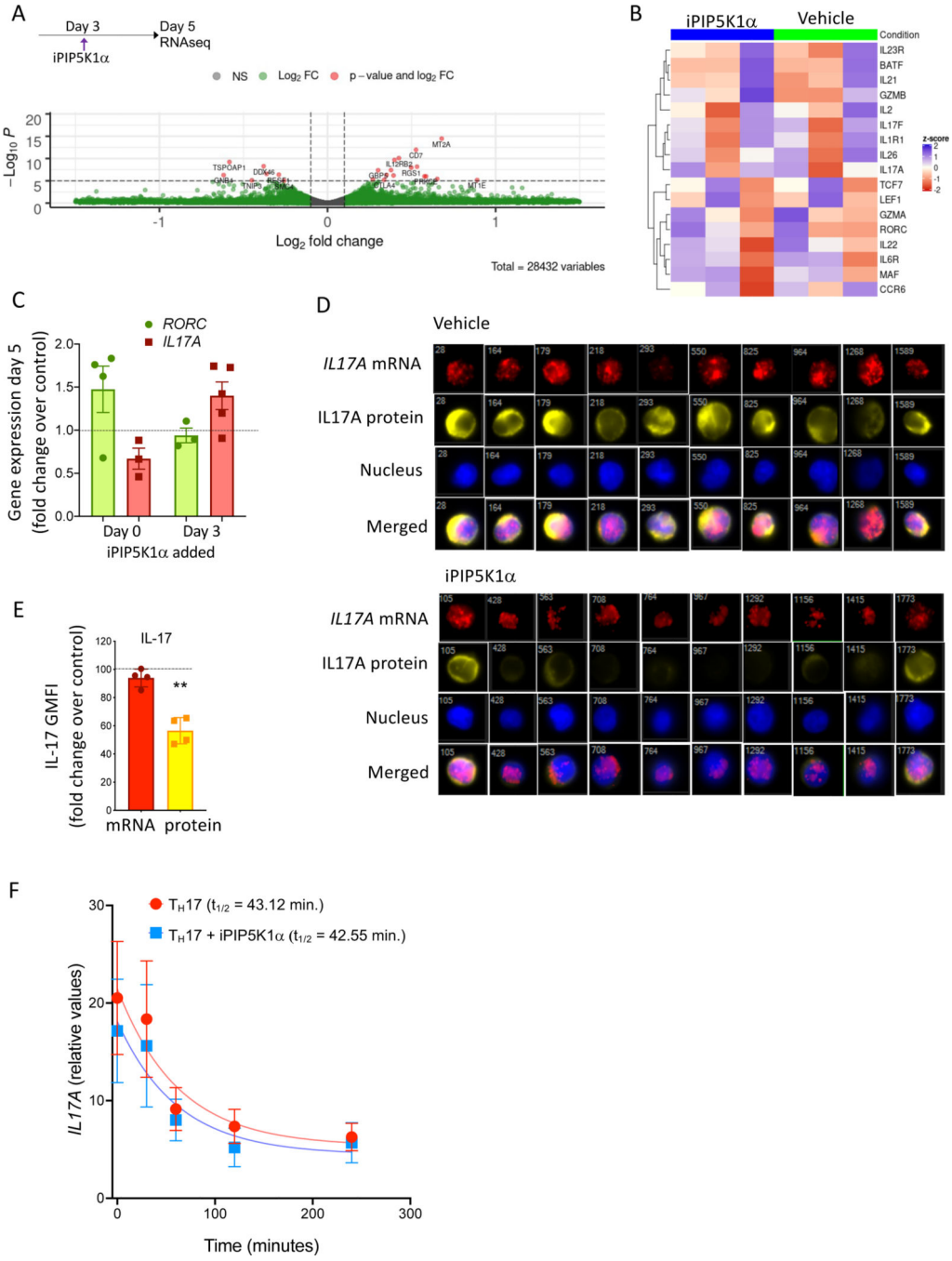

Fig. 4. PIP5K1α regulates IL-17A protein production post-transcriptionally.

(**A** and **B**) T_H17 cells were differentiated from naïve T cells as described for Fig. 1A. iPIP5K1α was added on day 3, and mRNA was extracted on day 5 for RNA-seq analysis. Data are from three donors. (A) Volcano plot showing differences in gene expression between the iPIP5K1α-treated and vehicle-treated control samples. The x-axis shows $\log_2$ values of the fold-changes in gene expression between the samples, whereas the y-axis shows -$\log_{10}$-transformed *P* values. Genes with adjusted *P* values < 0.05 and log-fold-change values >0.5 are colored in red. (B) Heatmap of T_H17 cell signature gene expression

in inhibitor-treated and control cells (there were no statistically significant differences). (**C**) T_H17 cells were differentiated and iPIP5K1α was added on days 0 or 3 of culture. On day 5, mRNA was extracted, and *RORC* and *IL17A* gene expression were determined by qPCR analysis. Data are expressed as the fold-change relative to the vehicle control condition for each donor and are from three to five donors. (**D** and **E**) T_H17 cells were differentiated, and iPIP5K1α was added on day 0. Imaging flow cytometry was used to analyze *IL17A* mRNA and IL-17A protein in both inhibitor-treated and vehicle-treated control cells. (D) Representative images selected at random from one donor. (E) The GMFI values for IL-17A protein and *IL17A* mRNA in the iPIP5K1α-treated cells as a percentage of the values for vehicle-treated cells. Data are from ~1000 cells per donor for four donors. Data in (C) and (E) were analyzed by one-sample *t* test against the hypothesized mean. (**F**) T_H17 cells were differentiated, and iPIP5K1α or vehicle was added on day 3. On day 5, Roadblock qPCR mRNA stability assays were performed, and the indicated half-lives of *IL17A* mRNA for each condition were determined by one-phase decay non-linear fit. Data are pooled from five individual donors. Data are means ± SD. $*P < 0.05$.

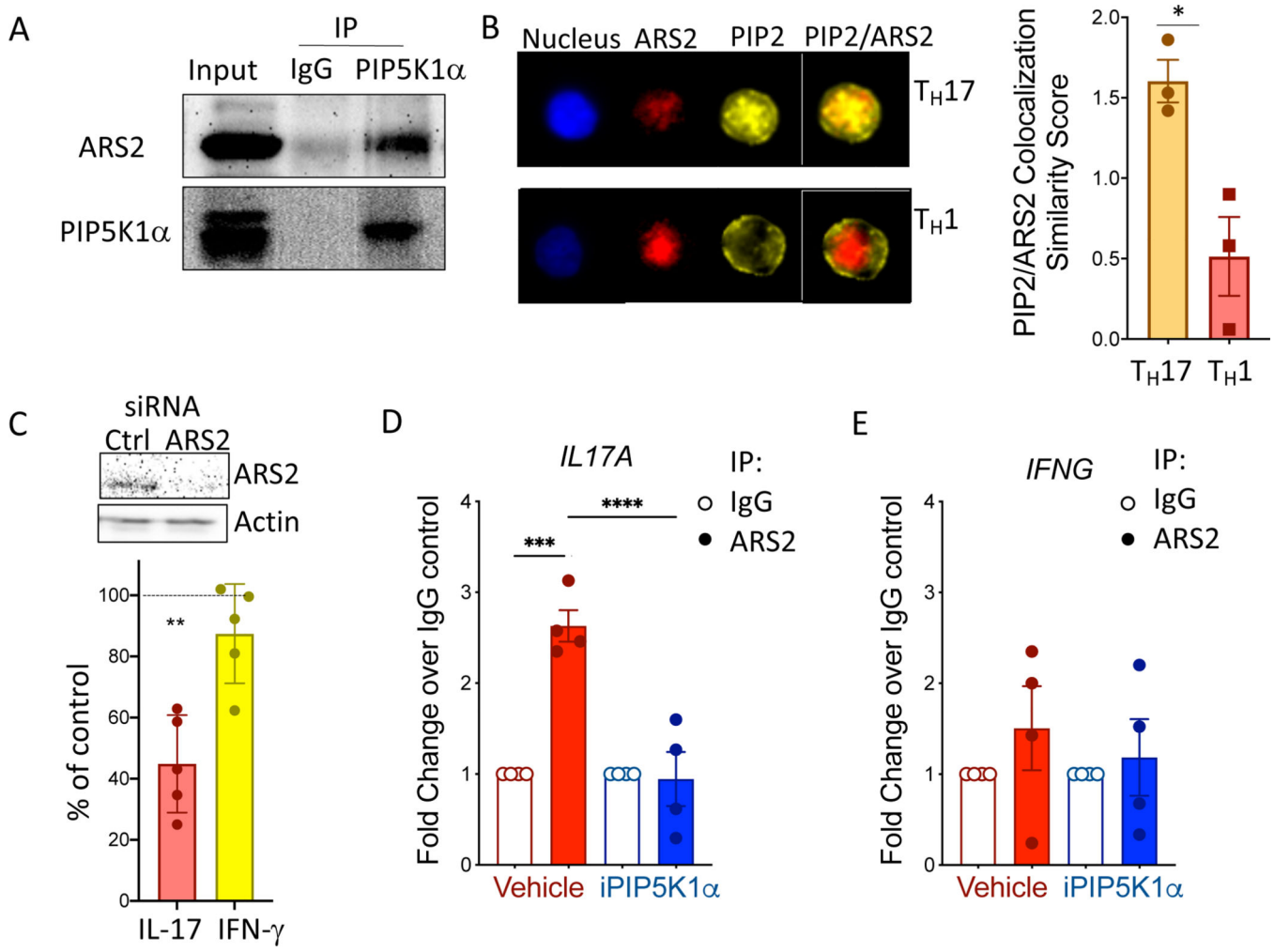

Fig. 5. PIP5K1α interacts with ARS2 to promote the translation of *IL17A* mRNA.

(**A**) Lysates of T_H17 cells generated as described for Fig. 1A were subjected to immunoprecipitation (IP) with anti-PIP5K1α or IgG control. Samples were then analyzed by Western blotting with antibodies against ARS2 and PIP5K1α. Data are representative of six donors. (**B**) Imaging flow cytometry analysis of ARS2 and PIP_2 in T_H17 and T_H1 cells. Left: Representative images. Right: Colocalization scores for ~1000 cells per donor for three donors. (**C**) Naïve T cells transfected with ARS2-specific siRNA or a scrambled siRNA control. Top: After 48 hours, samples were analyzed by Western blotting with antibodies against the indicated proteins. Bottom: On day 7 of culture under T_H17 conditions, the amounts of the indicated cytokines secreted by cells treated with ARS2-specific siRNA were normalized to those secreted by control cells for each donor, where 100% indicates no change. Data are from five donors. (**D** and **E**) T_H17 cells were differentiated for 6 days, with iPIP5K1α or vehicle added on day 3. The cells were subjected to RNAIP with anti-ARS2 or IgG as a control, which was followed by qPCR analysis of the relative amounts of *IL17A* (D) and *IFNG* (E) mRNAs. Dots represent individual donors (n=4), and values were normalized to those of the IgG-RIP control. Statistical analysis was performed by one-way ANOVA with multiple comparisons or by one-sample *t* test against the hypothesized mean

for data normalized to the control group. Data are means ± SD. *$P < 0.05$, ***$P < 0.001$, and ****$P < 0.0001$.